Title	Corrective Voltage Control Scheme Considering Demand Response and Stochastic Wind Power
Authors(s)	Rabiee, Abbas, Soroudi, Alireza, Mohammadi-Ivatloo, Behnam, Parniani, Mostafa
Publication date	2014-11
Publication information	Rabiee, Abbas, Alireza Soroudi, Behnam Mohammadi-Ivatloo, and Mostafa Parniani. "Corrective Voltage Control Scheme Considering Demand Response and Stochastic Wind Power" 29, no. 6 (November, 2014).
Publisher	Institute of Electrical and Electronics Engineers
Item record/more information	http://hdl.handle.net/10197/6115
Publisher's statement	(c) 2014 IEEE. Personal use of this material is permitted. Permission from IEEE must be obtained for all other users, including reprinting/ republishing this material for advertising or promotional purposes, creating new collective works for resale or redistribution to servers or lists, or reuse of any copyrighted components of this work in other works
Publisher's version (DOI)	10.1109/TPWRS.2014.2316018

Corrective Voltage Control Scheme Considering Demand Response and Stochastic Wind Power

Abbas Rabiee, Alireza Soroudi, *Member, IEEE*, Behnam Mohammadi-ivatloo, *Member, IEEE*, and Mostafa Parniani, *Senior Member, IEEE*

***Abstract*—This paper proposes a new approach for corrective voltage control (CVC) of power systems in presence of uncertain wind power generation and demand values. The CVC framework deals with the condition that a power system encounters voltage instability as a result of severe contingencies. The uncertainty of wind power generation and demand values is handled using scenario-based modeling approach. One of the features of the proposed methodology is to consider participation of demand-side resources as an effective control facility that reduces control costs. Active and reactive re-dispatch of generating units and involuntary load curtailment are employed along with the voluntary demand-side participation (demand response) as control facilities in the proposed CVC approach. The CVC is formulated as a multi-objective optimization problem. The objectives are ensuring a desired loading margin while minimizing the corresponding control costs. This problem is solved using ϵ-constraint method, and fuzzy satisfying approach is employed to select the best solution from the Pareto optimal set. The proposed control framework is implemented on the IEEE 118-Bus system to demonstrate its applicability and effectiveness.**

***Keywords*—Demand response (DR), loading margin (LM), scenario-based approach, voltage security, wind power generation, voltage control.**

NOMENCLATURE

A. Sets:

NB_{CVC}	Set of buses selected for the CVC program.
NG_{CVC}	Set of generating units that participate in the CVC program.
NG	Set of generating units.
NG_b	Set of generating units located at bus b.
NS	Set of scenarios.
NB	Set of system buses.
NL	Set of transmission lines.

B. Indices:

i	Index for generation units.
s	Index for scenarios.
b	Index for system buses.
ℓ	Index for transmission lines.

C. Parameters:

$(P/Q)^D_{b,s}$	Active/reactive power consumption of load connected to bus b at scenario s.
λ_{des}	Desired loading margin.
Y_{bj}/ϕ_{bj}	Magnitude/angle of bj^{th} element of admittance matrix at the post-contingency state.
$(P/Q)^G_{i,\max/\min}$	Max/minimum active/reactive power of generator i.
$\Delta(P/Q)^{G,up/down}_{i,\max}$	Maximum active power inc/decrement for generator i.
$\Delta(P/Q)^{DR/ILC}_{b,\max}$	Maximum active/reactive power decrement in DR/ILC program at bus b.
$S^{\max}_{\ell}$	Maximum transfer capacity of line ℓ.
$Q^w_{b,\max/\min}$	Max/minimum reactive power output of wind turbine at bus b
$V^{\max/\min}_b$	Max/minimum voltage at bus b.
v_m	Mean wind speed in m/s.
π_s	Probability of scenario s.
$\mu^{P/Q,up/down}_i$	Price offered by generator i to inc/decrease its active/reactive power schedule.
$\mu^{P/Q,DR/ILC}_b$	Price offered by demand b to decrease its active/reactive power schedule in the context of DR/ILC program.
$wp_{b,s}$	Percent of wind turbine capacity produced at bus b and scenario s.
$K_{G,i}$	Rate of change in active power generation of unit i.
$K_{D,b}$	Rate of load change at bus b.
$P^w_{b,r}$	Rated active power of wind turbine connected to bus b.
$(P/Q)^{G,sch}_i$	Scheduled active/reactive power of generator i.
v	Wind speed in m/s.

D. Variables:

$\Delta P^{G,up/down}_i$	Active power inc/decrement of generator i.
$P^w_{b,s}/Q^w_{b,s}$	Active/reactive wind power production injected to bus b in scenario s.
P^G_i	Active power production of generator i.
$\hat{P}^D_{b,s}/\hat{Q}^D_{b,s}$	Active/reactive power consumption of load connected to bus b in scenario s at loadability limit point.
$\hat{P}^G_{i,s}/\hat{Q}^G_{i,s}$	Active/reactive power production of generator i in scenario s at loadability limit.
$\Delta(P/Q)^{DR/ILC}_{b,s}$	Active/reactive power decrement in DR/ILC program at bus b in scenario s.
$S_{\ell,s}(.)$	Apparent power of line ℓ in scenario s.
λ_s	Loading margin in scenario s.
$\Delta Q^{G,up/down}_{i,s}$	Reactive power inc/decrement of generator i in scenario s.
$Q^G_{i,s}$	Reactive power production of generator i in scenario s.

A. Rabiee is with the Department of Electrical Engineering, Faculty of Engineering, University of Zanjan, Zanjan, Iran, (e-mail: rabiee@znu.ac.ir).

A. Soroudi (e-mail: alireza.soroudi@gmail.com).

B. Mohammadi-ivatloo is with the Faculty of Electrical and Computer Engineering, University of Tabriz, Tabriz, Iran (e-mail: mohammadi@ieee.org).

M. Parniani is with the Center of Excellence in Power System Control and Management (CEPSCM), Department of Electrical Engineering, Sharif University of Technology (SUT), Tehran, Iran (e-mail: parniani@sharif.edu).

$V_{b,s}/\theta_{b,s}$	Voltage magnitude/angle of bus b in scenario s.
$\hat{V}_{b,s}/\hat{\theta}_{b,s}$	Voltage magnitude/angle of bus b in scenario s at loadability limit point.

I. Introduction

In recent years voltage instability has received wide attention among power system utilities, due to the several reported incidents caused by this phenomenon [1], [2]. The growth of electrical energy demand, economic and environmental concerns in expanding generation and transmission capacities, and market pressure to reduce operating costs have forced power systems to operate ever closer to their voltage stability limits. Under such circumstances, there is possibility of voltage instability occurrence, and therefore, it has to be considered as an integral part of power system operation and planning studies. Also, the recent trends toward smart grids and increasing share of renewable energy resources in many power systems, have intensified the needs for powerful approaches for power system security enhancement [3], [4].

In order to restore voltage stability of power system, one had to curtail some of the system loads in case of heavy system loadings or occurrence of critical contingencies [5]. Nevertheless, forced load curtailment is undesirable for customers and the system operator should pay high penalties denoted as value of lost load (VLL). Demand Response (DR) program can be a good alternative for involuntary load curtailment (ILC), by curtailing the customer loads with their permissions. DR is defined as changes of customer loads from nominal value in response to price changes, incentive payments of operator or reliability problems [6], [7]. Beside the financial benefits of DR for customers (bill savings and incentive payments) and other market participants (lowering market clearing price and capacity requirement), DR program can be utilized for enhancing power system reliability and stability. The impact of DR program on power system reliability is investigated in [8]. Application of DR in enhancing frequency stability of power system is studied in [9] and [10]. Using DR programs for improvement of small-signal and transient stability of power systems with high wind power penetration are proposed in [11] and [12], respectively. An event-driven emergency DR scheme to enhance power system security has been proposed in [13]. With the increasing growth of wind power penetration in power systems, the effect of wind power in reactive power control is studied in [14], [15]. A new index titled reactive power loadability (Q-loadability) is proposed in [14] for finding the optimal location of reactive power compensation devices in distribution systems considering different wind power penetration levels. The effect of emergency demand response program (EDRP) and time of use program (TOU) programs on operating cost of a wind integrated distribution network is studied in [15]. An overview of the classic and advanced voltage control schemes along with voltage control practices around the world are provided in [16].

Corrective voltage control (CVC) is initiated in conditions that the system encounters voltage instability as a result of severe contingencies [17]. In this situation, CVC actions bring the post-contingency operating point to an equilibrium point with a sufficient loading margin (LM), immediately after occurrence of a contingency. LM is defined as the amount of load increase not arousing voltage instability or violation of operational constraints. An operating point is secure if its LM is more than a desired positive value. Otherwise, the system is insecure. Moreover, if the LM is negative (i.e the load demand is greater than the power generation), the system is unstable [18].

Satisfying power systems voltage security in the framework of preventive/corrective control is not a new problem and has been investigated in the literature [19], [18]. For instance, [19], after bringing an unstable operating point to a stable region in the context of CVC, first tries to satisfy a desired voltage stability margin, and then brings the operating point to a secure region where the operational constraints are satisfied. But, the proposed formulation in this paper satisfies both the voltage stability margin and the operational constraints in one step and in one optimization problem, resulting in better solutions. In [18], in spite of thoroughness of the technical work, the problem of controlling voltage security is not presented in a hierarchical framework to recognize what types of control measures are to be taken in different threatening conditions. Also, its formulation does not exploit load shedding as a fast and effective tool for providing voltage security.

This paper presents CVC as an optimization problem, considering the complete nonlinear model of the system; and hence, eliminates the above-mentioned problems with [19]. In contrast to [18], it provides further insight toward controlling voltage security in power systems, both technically and economically. It also uses probabilistic load shedding in the form of DR for CVC, which has not been addressed before in the literature [20]. In addition, noting the increasing penetration of wind power generation in nowadays power systems, scenario based approach [21] is adopted for appropriate modeling of intermittent wind power generation in the proposed CVC model. The proposed CVC approach is formulated as a multi-objective optimization problem. The objectives are maximizing LM and minimization of its corresponding CVC cost. This multi-objective problem is solved using ϵ-constraint method and the Pareto optimal set is obtained. Then, by employing fuzzy satisfying approach, the best solution is selected from this set. Given the above context, the contributions of this paper are:

1) To assess the effect of the intermittent wind power generation on CVC using a scenario based approach
2) To consider the total nonlinear model of the power system in optimized CVC
3) To model technical and economical aspects simultaneously by proposing a multi-objective optimization framework
4) To model the DR programs and customer choices in the required load shedding for CVC
5) To utilize ϵ-constraint method and fuzzy satisfying approach for solving and selecting the best compromising solution of the multi-objective optimization problem.

The rest of this paper is set out as follows. Section II describes CVC procedure. Section III presents the utilized uncertainty modeling approach, the problem formulation and its solution methodology. Simulation results are presented in Section IV. Finally, the findings of this work are summarized in Section V.

II. Corrective Voltage Control (CVC)

Based on the experience of Western Electricity Coordinating Council (WECC) [22], for secure operation of a power system from voltage security point of view, it is suggested to preserve specified LMs for both the base case and post-contingency conditions. If the system is unstable as a result of a severe contingency, fast control actions should be taken in order to

prevent voltage instability and provide voltage security. This kind of control is referred as corrective voltage control or emergency voltage control [23]. In this regard, the mission of CVC is to improve the LM from a negative value to a desired post-contingency value (λ_{des}), using fast remedial actions. These remedial controls are active power generation re-dispatch of fast-response generating units, reactive power generation re-dispatch of all dynamic VAR sources including synchronous generators and condensers, FACTS controllers' settings, switching of fast switchable capacitor banks/reactors, and load curtailment. To explain the CVC with more details, consider Fig. 1, which depicts PV curves of an arbitrary load bus for three states as follows:

Pre-contingency (curve (1))
Post-contingency - before applying CVC (curve (2))
Post-contingency - after applying CVC (curve (3))

The pre-contingency operating point A (with the demand of P_L^0) is located on curve (1). After occurrence of a severe contingency, the PV curve changes to curve (2). Thus, the LM becomes negative and the post-contingency equilibrium vanishes. Implementing the CVC will change the PV curve from curve (2) to curve (3); and hence the new operating point B is achieved, which is a stable and secure post-contingency equilibrium point. The loading parameter, λ_{des}, shown in Fig. 1, indicates the desired LM which should be ensured by implementing the CVC.

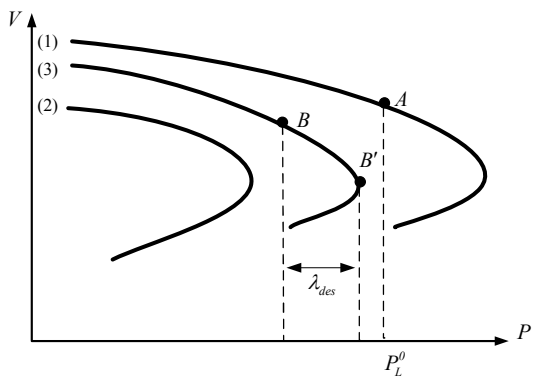

Fig. 1. Evolution of the operating points during the CVC step

III. Problem formulation

A. Uncertainty modeling of wind power and electric demand

The variation of wind power generation is an uncertain parameter which can be modeled probabilistically using historical data records of wind speed [21], [24]. In this paper, variation of wind speed, v, is modeled using Rayleigh probability density function (PDF) [25].

$$PDF(v) = (\frac{v}{c^2})\ exp[-(\frac{v^2}{2c^2})] \tag{1}$$

The generated power of a wind turbine in terms of wind speed is approximated as follows [24]:

$$P_b^w(v) = \begin{cases} 0 & \text{if } v \leq v_{in}^c \text{ or } v \geq v_{out}^c \\ \frac{v - v_{in}^c}{v_{rated}^c - v_{in}^c} P_{b,r}^w & \text{if } v_{in}^c \leq v \leq v_{rated} \\ P_{b,r}^w & \text{else} \end{cases} \tag{2}$$

where v_{in}^c, v_{rated}^c, and v_{out}^c are the cut-in, rated and cut-off speed of wind turbine, respectively. $P_{b,r}^w$ denotes rated power of the wind turbine installed at bus b. More accurate relations could also be used instead of the linear $P-V$ relation for the interval $v_{in}^c \leq v \leq v_{rated}$ [26]. Using the technique described in [24], [27], the PDF of wind speed is divided into several intervals, and the probability of falling into each interval is calculated. Each interval is given a mean value which is further used. Demand values are modeled using a normal distribution function with a known mean and variance. It is assumed that the load and wind power generation scenarios are independent so the scenarios are combined to construct the whole set of scenarios as follows [28].

$$\pi_s = \pi_w \times \pi_l \tag{3}$$

where π_w and π_l are the probabilities of the w-th wind and the l-th load scenarios, respectively. The total number of scenarios, i.e., NS, will be $l_n \times w_n$, where w_n, l_n are the number of wind and load states.

B. Formulation of the proposed CVC

The goal of the system operator is to optimize the expected values of two objective functions, namely, minimizing the cost of corrective voltage control and maximizing the loading margin of each scenario, while satisfying network's equality and inequality operational constraints. The equality constraints include AC power flow equations, and the inequality constraints consist of the limits of system variables (e.g. voltages, active and reactive powers, etc.). As noted in [18], the constraints should be considered for both the post-contingency operating point (i.e. point B in Fig. 1) and its corresponding loadability limit point (i.e. point B' in Fig. 1) to ensure the relation between the operating point and the critical point. Also, determination of control measures considering merely the operational constraints at the critical point may cause voltage violation in operating points with lower load levels [20]. Thus, the problem is inherently a multi-objective optimization problem. The vector of objective functions is described as follows.

$$\min \bar{f}(\bar{u_s}, \bar{x_s}, \bar{y_s}, s) \tag{4}$$
$$\bar{f}(\bar{u_s}, \bar{x_s}, \bar{y_s}, s) = [f_1(\bar{u_s}, \bar{x_s}, \bar{y_s}, s), -f_2(\bar{u_s}, \bar{x_s}, \bar{y_s}, s)]$$

where,

$$f_1(\bar{u_s}, \bar{x_s}, \bar{y_s}, s) = \sum_{i \in NG_{CVC}} \left(\mu_i^{P,up/down} \Delta P_i^{G,up/down}\right) \tag{5}$$
$$+ \sum_{s \in NS} \pi_s \left\{ \begin{array}{l} \sum_{i \in NG} \mu_i^{Q,up/down} \Delta Q_{i,s}^{G,up/down} \\ + \sum_{i \in NB_{CVC}} \mu_b^{P,DR/ILC} \Delta P_{b,s}^{DR/ILC} \\ + \sum_{i \in NB_{CVC}} \mu_b^{Q,DR/ILC} \Delta Q_{b,s}^{DR/ILC} \end{array} \right\}$$

$$f_2(\bar{u_s}, \bar{x_s}, \bar{y_s}, s) = \sum_{s \in NS} \pi_s \lambda_s \tag{6}$$

The negative sign before f_2 in right hand side of (4), maximizes f_2. Equation (5) is the expected cost of CVC. The first line in (5) represents the cost of active power re-dispatch of fast-response units. The second line is the expected cost of generating units' reactive power re-dispatch. Also, the third and the forth lines include the expected costs of active and reactive load curtailment performed by DR program, and the cost of ILC, respectively. The expected value of LM is given by (6). Besides, $\bar{u_s}, \bar{x_s}, \bar{y_s}$ are the vectors of control, state and dependent variables at the post-contingency operating point in scenario s, respectively. Detailed description of these variables

will be given later in this paper. The objective function in (4) is subject to the following constraints: For $\forall b \in NB, \forall s \in NS$:

$$\left(\sum_{i=1}^{NG_b} P_i^G\right) + P_{b,s}^w - \left(P_{b,s}^D - \Delta P_{b,s}^{DR} - \Delta P_{b,s}^{ILC}\right) = \tag{7}$$
$$V_{b,s} \sum_{j=1}^{NB} V_{j,s} Y_{bj} cos(\theta_{b,s} - \theta_{j,s} - \phi_{bj})$$
$$\left(\sum_{i=1}^{NG_b} Q_{i,s}^G\right) + Q_{b,s}^w - \left(Q_{b,s}^D - \Delta Q_{b,s}^{DR} - \Delta Q_{b,s}^{ILC}\right) = \tag{8}$$
$$V_{b,s} \sum_{j=1}^{NB} V_{j,s} Y_{bj} sin(\theta_{b,s} - \theta_{j,s} - \phi_{bj})$$
$$\forall i \in NG_{CVC}:$$
$$P_i^G = P_i^{G,sch} + \Delta P_i^{G,up} - \Delta P_i^{G,down} \tag{9}$$
$$0 \le \Delta P_i^{G,up} \le \Delta P_{i,max}^{G,up} \tag{10}$$
$$0 \le \Delta P_i^{G,down} \le \Delta P_{i,max}^{G,down} \tag{11}$$
$$\forall i \in NG; \forall s \in NS:$$
$$Q_{i,s}^G = Q_i^{G,sch} + \Delta Q_{i,s}^{G,up} - \Delta Q_{i,s}^{G,down} \tag{12}$$
$$P_{i,min}^G \le P_i^G \le P_{i,max}^G \tag{13}$$
$$Q_{i,min}^G \le Q_{i,s}^G \le Q_{i,max}^G \tag{14}$$
$$\forall i \in NG; \forall s \in NS, \forall b \in NB, \forall \ell \in NL:$$
$$0 \le \Delta Q_{i,s}^{G,up} \le \Delta Q_{i,max}^{G,up} \tag{15}$$
$$0 \le \Delta Q_{i,s}^{G,down} \le \Delta Q_{i,max}^{G,down} \tag{16}$$
$$0 \le \Delta P_{b,s}^{DR} \le \Delta P_{b,s}^{DR,max} \tag{17}$$
$$0 \le \Delta Q_{b,s}^{DR} \le \Delta Q_{b,s}^{DR,max} \tag{18}$$
$$0 \le \Delta P_{b,s}^{ILC} \le \Delta P_{b,s}^{ILC,max} \tag{19}$$
$$0 \le \Delta Q_{b,s}^{ILC} \le \Delta Q_{b,s}^{ILC,max} \tag{20}$$
$$V_b^{min} \le V_{b,s} \le V_b^{max} \tag{21}$$
$$|S_{\ell,s}(V,\theta,s)| \le S_\ell^{max} \tag{22}$$

$\forall b \in NB; \forall s \in NS:$

$$\left(\sum_{i=1}^{NG_b} \hat{P}_{i,s}^G\right) + P_{b,s}^w - \hat{P}_{b,s}^D = \tag{23}$$
$$\hat{V}_{b,s} \sum_{j=1}^{NB} \hat{V}_{j,s} Y_{bj} cos(\hat{\theta}_{b,s} - \hat{\theta}_{j,s} - \phi_{bj})$$
$$\left(\sum_{i=1}^{NG_b} \hat{Q}_{i,s}^G\right) + Q_{b,s}^w - \hat{Q}_{b,s}^D = \tag{24}$$
$$\hat{V}_{b,s} \sum_{j=1}^{NB} \hat{V}_{j,s} Y_{bj} sin(\hat{\theta}_{b,s} - \hat{\theta}_{j,s} - \phi_{bj})$$

$$\hat{P}_{i,s}^G = \min\left(P_i^{G,max}, (1 + K_{G,i}\lambda_s) P_i^G\right) \tag{25}$$
$$\hat{P}_{b,s}^D = (1 + K_{D,b}\lambda_s)\left(P_{b,s}^D - \Delta P_{b,s}^{DR} - \Delta P_{b,s}^{ILC}\right) \tag{26}$$
$$\hat{Q}_{b,s}^D = (1 + K_{D,b}\lambda_s)\left(Q_{b,s}^D - \Delta Q_{b,s}^{DR} - \Delta Q_{b,s}^{ILC}\right) \tag{27}$$
$$0 \le P_{b,s}^w \le wp_{b,s} * P_{b,r}^w \tag{28}$$
$$Q_{b,min}^w \le Q_{b,s}^w \le Q_{b,max}^w \tag{29}$$

Finally $\forall b \in NB_G, \forall s \in NS, \forall i \in NG$:

$$P_{i,min}^G \le \hat{P}_{i,s}^G \le P_{i,max}^G \tag{30}$$
$$Q_{i,min}^G \le \hat{Q}_{i,s}^G \le Q_{i,max}^G \tag{31}$$
$$V_b^{min} \le \hat{V}_{b,s} \le V_b^{max} \tag{32}$$
$$\hat{V}_{b,s} = V_{b,s} = V_b \tag{33}$$
$$\lambda_s \ge \lambda_{des} > 0 \tag{34}$$

Constraints (7)-(22) correspond to the post-contingency secure operating point (point B in Fig. 1), whereas (23)-(32) correspond to the post-contingency loadability limit point (point $\acute{B}$ in Fig. 1). It is worth mentioning that (33) guarantees feasibility of the post-contingency operating point (point B in Fig. 1) and a trajectory from point B leading to point $\acute{B}$ in effect of load increment [29]. Also, (34) ensures the desired LM (i.e. λ_{des}) for all scenarios. The desired LM is set by the network operator. The sets of control, state and dependent variables are described as follows.

$$\bar{u}_s = \begin{bmatrix} V_b & b \in NG \\ \lambda_s & s \in NS \\ \Delta P_i^{G,up/down} & i \in NG_{CVC} \\ P_{b,s}^w, Q_{b,s}^w & b \in NB_w; s \in NS \\ \Delta P_{b,s}^{DR}, \Delta Q_{b,s}^{DR} & b \in NB_{CVC}; s \in NS \\ \Delta P_{b,s}^{ILC}, \Delta Q_{b,s}^{ILC} & b \in NB_{CVC}; s \in NS \end{bmatrix} \tag{35}$$
$$\bar{x}_s = \begin{bmatrix} V_{b,s}, \hat{V}_{b,s}, \theta_{b,s}, \hat{\theta}_{b,s} & b \in NB, s \in NS \end{bmatrix} \tag{36}$$
$$\bar{y}_s = \begin{bmatrix} \Delta Q_{i,s}^{G,up/down}, \hat{Q}_{i,s}^G & i \in NG, s \in NS \\ S_{\ell,s} & \ell \in NL, s \in NS \end{bmatrix} \tag{37}$$

The proposed model utilizes a two-stage stochastic modeling technique. In this approach, the decision variables are divided into two different categories, namely, **here and now** & **wait and see**. The values of **wait and see** variables differ from one scenario to another, while the values of **here and now** variables are the same for all scenarios. This means that the **here and now** decisions are made prior to realization of uncertain parameters and the **wait and see** variables are calculated to be applied posterior to the realization of uncertain parameters (i.e. after realization of the corresponding scenario). The type of the decision variables are identified in the following:

Here and now decision variables (D_{HN}):

$$D_{HN} \in \left\{\Delta P_i^{G,up/down}, V_b\right\} \tag{38}$$

Wait and see decision variables (D_{WS}):

$$D_{WS} \in \left\{ \begin{array}{c} P_{b,s}^w, Q_{b,s}^w, \lambda_s \\ \Delta P_{b,s}^{DR}, \Delta Q_{b,s}^{DR} \\ \Delta P_{b,s}^{ILC}, \Delta Q_{b,s}^{ILC} \end{array} \right\} \tag{39}$$

C. Solution Procedure

Various methods are available to solve multi-objective optimization problems such as weighted sum approach, ϵ-constraint method, evolutionary algorithms, etc [30]. In this paper, the proposed multi-objective model of the CVC is solved using ϵ-constraint method, which is an efficient technique to solve problems with non-convex Pareto front. This method generates single objective subproblems, by transforming all but one objective into constraints. The upper bounds of these constraints are given by the epsilon-vector and by varying it, the Pareto front can be obtained. The concept of Pareto optimality is explained

in [27]. Also, in order to choose the best solution among the obtained Pareto optimal set, fuzzy satisfying approach [31] is adopted in this paper. This approach is described in [27].

IV. Simulation Results

The proposed algorithm is implemented in General Algebraic Modeling System (GAMS) [32] environment and solved by SNOPT solver [33]. This section presents the study results conducted on the IEEE 118-bus test system. The data of this system is given in [34]. In order to determine the LM, the loads are increased evenly with constant power factor characteristic. Active powers of the generators, not hitting their upper limits in the base-case, are also increased evenly. The costs of up and down re-dispatching active and reactive powers of generating units are assumed to be 125%, 25%, 12.5%, 2.5% of the base case locational marginal price (LMP) of the buses connected to generating units, respectively. The cost of ILC at each bus is considered to be 100 times of LMP of that bus. The costs paid to participants of DR programs to deploy their load reduction in a given bus are also assumed to be 10 times of the LMP of that bus. The desired post-contingency LM is considered to be 10%.

This study investigates a double-contingency case, i.e. simultaneous outages of the line L_{1-3} (between the buses B_1 and B_3) and the generator G_5 (located at bus B_{10}). This event leads to voltage collapse in the system. Hence, the CVC is taken to restore voltage stability, and to provide voltage security in the post-contingency condition. The CVC improves the LM from -8.1% to the desired post-contingency value of 10%. It is assumed that utmost 5% of the demand at buses B_{44}, B_{45}, B_{47}, B_{48}, $B_{50}-B_{53}$, B_{57}, B_{58}, $B_{82}-B_{84}$, B_{86} and B_{88} are selected for DR program. Also, it is assumed that the fast-response generation units are those located at buses B_{24}, B_{25}, B_{46}, B_{49}, $B_{54}-B_{56}$, B_{85}, B_{87}, B_{89} and B_{90}.

It is also assumed that five wind farms exist in this system, which are located at buses B_{14}, B_{51}, B_{57}, B_{102} and B_{115}. The total wind generation capacity of each wind farm is assumed to be $200MW$. The wind and load scenarios are combined and the overall wind-load scenarios along with the corresponding wind/load percentages and probabilities are given in Table I. Initial schedule of active power generations are given in Fig. 2.

In order to solve the multi-objective CVC problem by ϵ-constraint method, maximum and minimum values of the expected LM (i.e. f_2) are calculated, which are equal to 0.3267 and 0.1000, respectively. These border values are achieved by maximizing and minimizing f_2 individually as the objective function of CVC. Then, by assuming f_2 as a constraint of the CVC (in the form of $f_2 \geq \epsilon$), lower bound of f_2 (i.e. ϵ) varies from 0.1000 to 0.3267 and f_1 is minimized as the sole objective function of CVC. Correspondingly, the Pareto optimal front of the two objective functions is derived, which is depicted in Fig 3. This Pareto front consists of 40 Pareto optimal solutions.

Table II shows the values of both objective functions for all 40 Pareto optimal solutions. Among these optimal solutions, *Solution#1* is the minimum cost case, with the cost equals to \$10431.511 and the LM of 10%. Also, *Solution#40* is the maximum LM case, where the LM is 0.3267 and the CVC cost is \$841307.979. Active power redispatch of the fast-response generating units are give in Fig. 4. For this solution, the wind power scenario-based active and reactive power dispatchs are given in Table III. The consequent probabilistic schedule of DR and ILC for different scenarios are given in Table IV.

As explained in Section III, in order to select the best solution among the obtained Pareto optimal set, fuzzy satisfying method is utilized here. It is evident from the last column of Table II that the best solution is *Solution#29*, with the maximum weakest membership function of 0.7890. The corresponding CVC cost and LM are equal to \$175161.218 and 0.2789, respectively. Figure 5 gives the redispatch of fast-response generating units for this case. Besides, the voltage magnitudes of generator buses for both *Solution#1* and *Solution#29* are given in Fig. 6. The active and reactive power output of wind farms in this case, are given in Table V. Also, the resulting DR and ILC schedules for this case are given in Table VI.

TABLE I. The wind-load scenarios and their probabilites

	load(%)	wind(%)	π_s
s_1	98	100	0.015
s_2	100	100	0.070
s_3	102	100	0.015
s_4	98	50	0.120
s_5	100	50	0.560
s_6	102	50	0.120
s_7	98	0	0.015
s_8	100	0	0.070
s_9	102	0	0.015

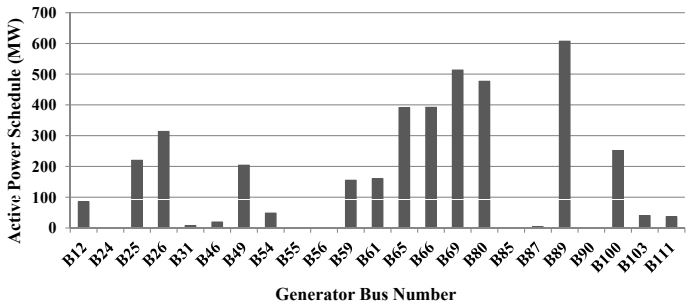

Fig. 2. Initial dispatch of active power generations (MW)

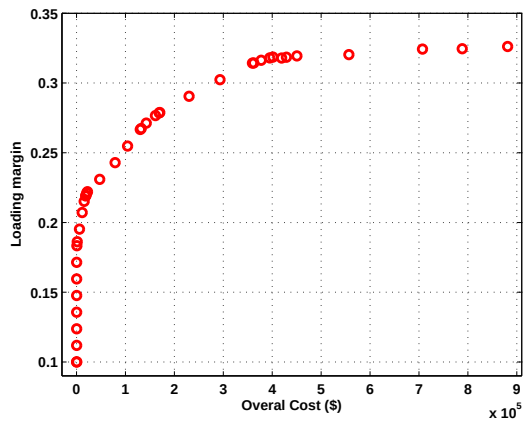

Fig. 3. The Pareto optimal front of the two objective functions

The expected cost for *Solution#29* is \$175161.218 , which is much greater than the corresponding cost of \$10431.511 for *Solution#1*. On the other hand, the LM in the former is 0.2789, which is greater than the 0.1000 in the latter. Also, for *Solution#29* the sum of expected DR and ILC schedules are 6.29 MW and 188.29 MW, respectively. While these values

TABLE II. THE PARETO OPTIMAL SOLUTIONS

Solution #(k)	f_1 ($)	f_2	$\frac{f_1^{max}-f_k}{f_1^{max}-f_1^{min}}$	$\frac{f_2^{min}-f_k}{f_2^{min}-f_2^{max}}$	Min
1	10431.511	0.1000	1.0000	0.0000	0.0000
2	10562.983	0.1004	0.9998	0.0017	0.0017
3	10563.115	0.1118	0.9998	0.0520	0.0520
4	10569.949	0.1236	0.9998	0.1040	0.1040
5	10580.599	0.1354	0.9998	0.1560	0.1560
6	10672.896	0.1472	0.9997	0.2080	0.2080
7	10748.059	0.1589	0.9996	0.2600	0.2600
8	11120.455	0.1707	0.9992	0.3120	0.3120
9	11801.023	0.1800	0.9984	0.3530	0.3530
10	12390.736	0.1825	0.9976	0.3640	0.3640
11	12406.505	0.1837	0.9976	0.3691	0.3691
12	12737.061	0.1848	0.9972	0.3739	0.3739
13	13112.559	0.1856	0.9968	0.3776	0.3776
14	18691.916	0.1943	0.9901	0.4160	0.4160
15	26448.570	0.2061	0.9807	0.4680	0.4680
16	30360.447	0.2129	0.9760	0.4980	0.4980
17	35470.611	0.2179	0.9699	0.5200	0.5200
18	36367.421	0.2201	0.9688	0.5296	0.5296
19	37324.050	0.2210	0.9676	0.5337	0.5337
20	37756.529	0.2213	0.9671	0.5352	0.5352
21	38426.818	0.2217	0.9663	0.5369	0.5369
22	58819.375	0.2297	0.9418	0.5720	0.5720
23	92731.830	0.2415	0.9009	0.6240	0.6240
24	121278.919	0.2533	0.8666	0.6760	0.6760
25	146924.208	0.2651	0.8357	0.7280	0.7280
26	154405.201	0.2717	0.8267	0.7575	0.7575
27	160232.543	0.2741	0.8197	0.7677	0.7677
28	174941.335	0.2768	0.8020	0.7800	0.7800
29	**175161.218**	**0.2789**	**0.8017**	**0.7890**	**0.7890**
30	192337.631	0.2831	0.7811	0.8076	0.7811
31	227002.052	0.2886	0.7393	0.8320	0.7393
32	286672.194	0.3004	0.6675	0.8840	0.6675
33	348531.071	0.3122	0.5931	0.9360	0.5931
34	346772.318	0.3139	0.5952	0.9437	0.5952
35	362514.944	0.3158	0.5763	0.9517	0.5763
36	383521.825	0.3181	0.5510	0.9618	0.5510
37	399504.032	0.3192	0.5317	0.9667	0.5317
38	443335.754	0.3209	0.4790	0.9743	0.4790
39	632271.786	0.3240	0.2516	0.9880	0.2516
40	841307.979	0.3267	0	1	0

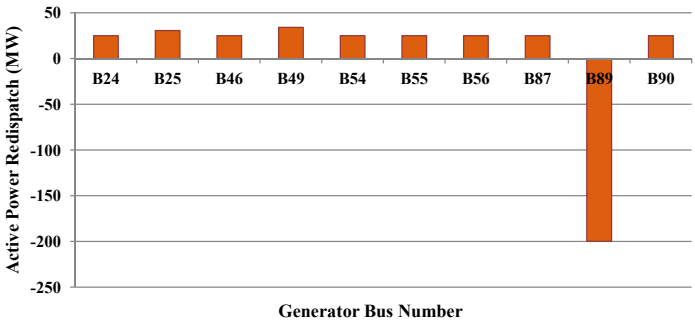

Fig. 4. Active power redispatch of fast-response generating units for *Solution#1*

are 0.79 MW and 6.18 MW, respectively, for *Solution#1*. The considerable difference between the expected costs for these two solutions, is mainly due to employing a large amount of expensive ILC, to obtain the LM of 0.2789 in *Solution#29*.

TABLE III. ACTIVE (MW) AND REACTIVE ($MVAr$) POWER GENERATION OF WIND FARMS IN DIFFERENT SCENARIOS FOR SOLUTION#1

	Bus	s_1	s_2	s_3	s_4	s_5	s_6	s_7	s_8	s_9
$P^w_{b,s}$	B_{14}		31.38	79.28	0	31.38	79.7			
	B_{115}		43.28	73.63	0	43.28	73.18			
$Q^w_{b,s}$	B_{14}	132.74	64.95	55.7	132.74	64.95	55.59	132.74	3.01	-1.61
	B_{51}	139.73	-48.72	-47.43	139.73	-48.72	-47.43	-50	30.06	31.72
	B_{57}	-28.23	94.35	96.15	-28.23	94.35	96.15	101.9	27.15	28.93
	B_{102}	37.81	31.69	38.34	37.81	31.69	35.22	37.81	24.21	27.68
	B_{115}	150	131.19	121.85	150	131.19	121.96	150	44.33	44.88

TABLE IV. DR AND ILC SCHEDULES IN DIFFERENT SCENARIOS FOR SOLUTION#1

	$\Delta P^{DR}_{b,s}$ (MW)						$\Delta P^{ILC}_{b,s}$ (MW)									
	B_{47}	B_{48}	B_{51}	B_{57}	B_{82}	B_{88}	B_1	B_2	B_3	B_7	B_{11}	B_{12}	B_{13}	B_{14}	B_{41}	B_{117}
s_8	1.7	1	0.85	0.6	2.7	2.4	9.4	19.15	0	0	0	0	15.03	0	0	15.75
s_9	1.7	1	0.85	0.6	2.7	2.4	10.28	20	11.52	11.66	10.6	13.78	28.27	6.02	3.19	20

In this work, the locations of wind turbines in the grid are priorly known. In case the optimal locations of wind turbines are to be determined, there exist some efficient methods in the literature to find them [35].

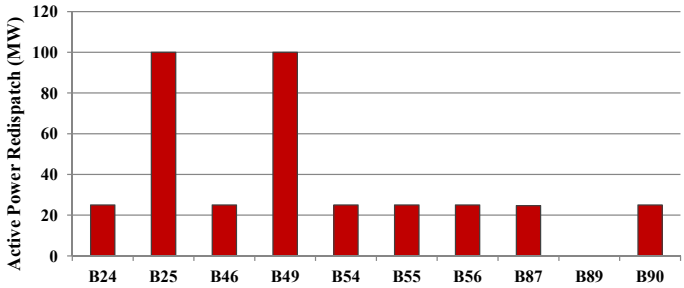

Fig. 5. Active power redispatch of fast-response generating units for *Solution#29* (MW)

TABLE V. ACTIVE (MW) AND REACTIVE ($MVAr$) POWER GENERATION OF WIND FARMS IN DIFFERENT SCENARIOS FOR SOLUTION#29

	Bus	s_1	s_2	s_3	s_4	s_5	s_6	s_7	s_8	s_9
$P^w_{b,s}$	B_{14}	140.12	200	200	100	100	100	0	0	0
	B_{51}	0	0	0	0	8.28	87.17	0	0	0
	B_{115}	0	12.72	102.77	41.9	100	100	0	0	0
$Q^w_{b,s}$	B_{14}	-10.56	-15.74	-15.62	4.87	3.54	8.57	0.15	-5.05	-4.23
	B_{51}	130.92	131.1	132.02	130.92	127.84	100.4	103.16	109.06	114.94
	B_{57}	116.84	118.47	120.5	116.84	118.37	120.97	122	122.3	122.61
	B_{102}	-45	-46.7	-42.97	-43.79	-46.24	-43.7	-50	-50	-49.36

A. *Value of stochastic solution*

It is obvious that using deterministic model results in simpler formulation and lower problem size in comparison with the stochastic models. In order to give an insight about the decisions made by two methods, the following studies are carried out.

Expected Value (EV) solution: In this case all of the random variables are replaced by the corresponding expected values (mean values of different scenarios) and the resulting deterministic problem is solved. The obtained objective function value is indicated as EV solution.

Stochastic solution (SS) or recourse problem (RP): the stochastic problem is solved considering all of the scenarios. The obtained objective function is called RP.

Expected outcome of using the expected value (EEV): In this case we have fixed the first stage variables with the results obtained from deterministic case (i.e. the results obtained from EV solution) and the stochastic program is solved considering the scenarios. EEV represents the true cost of the deterministic solution.

The value of stochastic solution (VSS) is calculated by subtracting the RP from the EEV as follows [36]:

$$VSS = EEV - RP \tag{40}$$

Table VII compares the obtained best compromise solution using the three mentioned methods. The VSS for cost is equal to $35,014.982 which indicates the extra cost of using deterministic method instead of the stochastic model.

V. CONCLUSION

In this paper, a probabilistic methodology is proposed for corrective voltage control (CVC) of power systems. The proposed CVC aims to employ demand response (DR) along with other resources as an effective tool to avoid voltage collapse and provides a desired post-contingency loading margin (LM). It considers the uncertainties associated with demand values and wind power generation. The uncertainties are modeled using scenario-based approach. The CVC problem is formulated as a

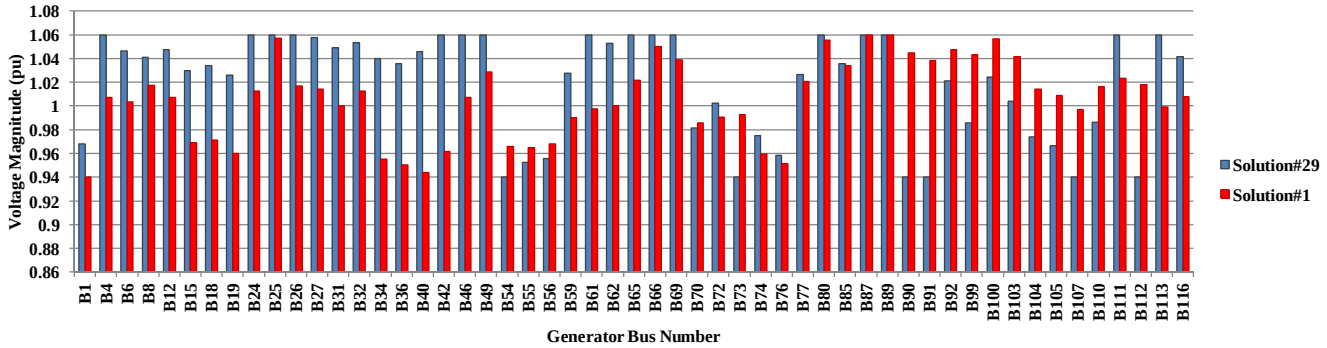

Fig. 6. Voltage magnitude of generator buses (pu), for solutions #1 and #29

TABLE VI. DR AND ILC SCHEDULES (MW) IN DIFFERENT SCENARIOS FOR SOLUTION#29

	Bus	s_1	s_2	s_3	s_4	s_5	s_6	s_7	s_8	s_9
$\Delta P^{DR}_{b,s}$	B_{47}	0	1.7	1.7	0	1.7	1.7	1.7	1.7	1.7
	B_{48}	0	1	1	0	1	1	1	1	1
	B_{51}	0	0.85	0.85	0	0.85	0.85	0.85	0.85	0.85
	B_{57}	0	0.6	0.6	0	0.6	0.6	0.6	0.6	0.6
	B_{82}	2.7	2.7	2.7	2.7	2.7	2.7	2.7	2.7	2.7
	B_{88}	0	0	0	0	0	2.4	2.4	2.4	2.4
$\Delta P^{ILC}_{b,s}$	B_1	0	0	0	0	0	0	0	0	0.39
	B_2	0	0	0	0	0	0	14.01	17.61	20
	B_3	0	0	0	0	0	0	9.47	18.27	22.8
	B_6	0	0	0	0	0	0	0	2.63	0
	B_7	0	0	0	0	0	0	0	18.99	18.92
	B_{11}	0	0	0	0	0	0	6.82	27.18	39.13
	B_{12}	0	0	0	0	0	0	10.75	10.31	17.55
	B_{13}	0	0	0	0	0	0	24.43	30.74	34
	B_{14}	0	0	0	0	0	0	0	10.69	14
	B_{16}	0	0	0	0	0	0	0	5.59	9.74
	B_{19}	0	0	0	0	0	0	0	0	4.26
	B_{20}	0	0	0	0	0	0	0	0	1.75
	B_{29}	0	0	0	0	0	0	0	10.93	15.05
	B_{33}	0	0	0	0	0	0	0	0	8.49
	B_{34}	37.79	32.87	27.67	38.64	37.36	42.39	45.05	33.9	25.64
	B_{36}	0	0	0	0	0	0	0	0	0
	B_{39}	0	0	0	0	0	0	0	0	6.65
	B_{41}	0	0	0	0	0	0	0	0	8.12
	B_{70}	0	0	0	0	0	0	5.29	0	0
	B_{74}	36.03	37.58	38.59	35.83	37.39	39.19	33.23	34.07	34.91
	B_{92}	45.66	44.42	33.13	42.8	40.41	38.33	22.93	25.84	25.98
	B_{93}	12	12	12	12	12	12	12	12	12
	B_{94}	0	0	0	0	0	0	7.36	7.7	9.48
	B_{95}	0	11.6	19.91	0	15.7	15.31	42	42	42
	B_{101}	22	22	22	22	22	22	22	22	22
	B_{102}	5	5	5	5	5	5	5	5	5
	B_{105}	0	0	0	0	0	0	0	0	1.06
	B_{110}	0	0	0	0	0	0	0	0	0.25
	B_{112}	0	0	0	0	0	0	0	0.12	13.18
	B_{117}	0	0	0	0	0	0	20	20	20
	B_{118}	0	0	0	0	0	0	12.78	15.96	19.3

TABLE VII. TOTAL COST AND LOADING MARGINS USING DIFFERENT UNCERTAINTY CONSIDERATION METHODS.

Method	EV	RP	EEV
Expected total cost	1700191.9	175161.2	210176.2
Expected loading margin	0.2788	0.2789	0.2889

multi-objective optimization problem. The objective functions are satisfying a desired expected LM and minimization of its corresponding expected CVC cost. This problem is solved using ϵ-constraint technique, to achieve the corresponding Pareto optimal set. Then, by using the Fuzzy satisfying method, the best solution is selected among the optimal set. The proposed approach is implemented on IEEE 118-bus test system, by simulation of a double contingency case. Numerical results show that in order to attain higher values of LM, more CVC cost is imposed. Hence, the system operator should make fair compromise between the desired LM and its corresponding CVC cost. The presented results show the effectiveness of the proposed probabilistic approach, to deal with the corrective voltage control of power systems.

REFERENCES

[1] C. Canizares *et al.*, "Voltage stability assessment: concepts, practices and tools," *IEEE/PES power system stability subcommittee special publication*, no. SP101PSS, August 2002.

[2] A. Rabiee and M. Parniani, "Voltage security constrained multi-period optimal reactive power flow using benders and optimality condition decompositions," *IEEE Transactions on Power Systems*, vol. 28, no. 2, pp. 696–708, 2013.

[3] M. Ortega-Vazquez and D. Kirschen, "Assessing the impact of wind power generation on operating costs," *IEEE Transactions on Smart Grid*, vol. 1, no. 3, pp. 295–301, 2010.

[4] A. Saber and G. Venayagamoorthy, "Efficient utilization of renewable energy sources by gridable vehicles in cyber-physical energy systems," *IEEE Systems Journal*, vol. 4, no. 3, pp. 285–294, 2010.

[5] C. Affonso, L. da Silva, F. Lima, and S. Soares, "Mw and *MVar* management on supply and demand side for meeting voltage stability margin criteria," *IEEE Transactions on Power Systems*, vol. 19, no. 3, pp. 1538–1545, 2004.

[6] U. D. of Energy, "Benefits of demand response in electricity markets and recommendations for achieving them," *A report to the United States cogress*, February 2006.

[7] P. Wang, Y. Ding, and L. Goel, "Reliability assessment of restructured power systems using optimal load shedding technique," *Generation, Transmission Distribution, IET*, vol. 3, no. 7, pp. 628–640, 2009.

[8] L. Goel, Q. Wu, and P. Wang, "Reliability enhancement of a deregulated power system considering demand response," in *IEEE PES Gen. Meet.*, 2006, pp. 1–6.

[9] J. A. Short, D. G. Infield, and L. L. Freris, "Stabilization of grid frequency through dynamic demand control," *IEEE Transactions on Power Systems*, vol. 22, no. 3, pp. 1284–1293, August 2007.

[10] L.-R. Chang-Chien, L. N. An, T.-W. Lin, and W.-J. Lee, "Incorporating demand response with spinning reserve to realize an adaptive frequency restoration plan for system contingencies," *IEEE Transactions on Smart Grid*, vol. 3, no. 3, pp. 1145–1153, Sept 2012.

[11] W. Hu, C. Su, Z. Chen, and B. Bak-Jensen, "Small signal stability improvement of power systems using optimal load responses in competitive electricity markets," in *46th International Universities' Power Engineering Conference*, 2011, pp. 1–6.

[12] ——, "Power system transient stability improvement using demand side management in competitive electricity markets," in *Proceedings of the 9th International Conference European Energy Market (EEM 2012)*, 2012, pp. 1–8.

[13] Y. Wang, I. Rahimi-Pordanjani, and W. Xu, "An event-driven demand response scheme for power system security enhancement," *IEEE Transactions on Smart Grid*, vol. 2, no. 1, pp. 23–29, March 2011.

[14] N. Roy, H. Pota, and M. Hossain, "Reactive power management of distribution networks with wind generation for improving voltage stability," *Renewable Energy*, vol. 58, no. 0, pp. 85 – 94, 2013.

[15] K. D. Mistry and R. Roy, "Impact of demand response program in wind integrated distribution network," *Electric Power Systems Research*, vol. 108, no. 0, pp. 269 – 281, 2014.

[16] M. Eremia and M. Shahidehpour, *Handbook of Electrical Power System Dynamics: Modeling, Stability, and Control*. Wiley. com, 2013, vol. 92.

[17] L. Wu, M. Shahidehpour, and C. Liu, "Mip-based post-contingency corrective action with quick-start units," *IEEE Transactions on Power Systems*, vol. 24, no. 4, pp. 1898–1899, 2009.

[18] W. Rosehart, C. Canizares, and V. Quintana, "Multiobjective optimal power flows to evaluate voltage security costs in power networks," *IEEE Transactions on Power Systems*, vol. 18, no. 2, pp. 578–587, 2003.

[19] Z. Feng, V. Ajjarapu, and D. Maratukulam, "A comprehensive approach for preventive and corrective control to mitigate voltage collapse," *IEEE Transactions on Power Systems*, vol. 15, no. 2, pp. 791 –797, may 2000.

[20] A. Rabiee, M. Parvania, M. Vanouni, M. Parniani, and M. Fotuhi-Firuzabad, "Comprehensive control framework for ensuring loading margin of power systems considering demand-side participation," *Generation, Transmission Distribution, IET*, vol. 6, no. 12, pp. 1189–1201, 2012.

[21] A. Soroudi, "Taxonomy of uncertainty modeling techniques in renewable energy system studies," in *Large Scale Renewable Power Generation*. Springer Singapore, 2014, pp. 1–17.

[22] V. Ajjarapu and A. P. S. Meliopoulos, *Preventing Voltage Collapse with Protection Systems that Incorporate Optimal Reactive Power Control*. Final Project Report PSERC Publication 08-20, Oct 2008.

[23] T. V. Cutsem and C. Vournas, *Voltage Stability of Electric Power Systems*. Springer, Nov. 1998.

[24] A. Soroudi, "Possibilistic-scenario model for dg impact assessment on distribution networks in an uncertain environment," *IEEE Transactions on Power Systems*, vol. 27, no. 3, pp. 1283–1293, Aug 2012.

[25] A. Rabiee and A. Soroudi, "Stochastic multiperiod opf model of power systems with hvdc-connected intermittent wind power generation," *IEEE Transactions on Power Delivery*, vol. 29, no. 1, pp. 336–344, 2014.

[26] H. Willis and W. Scott, *Distributed power generation: planning and evaluation*. CRC Press, 2000, vol. 10.

[27] A. Soroudi, B. Mohammadi-Ivatloo, and A. Rabiee, "Energy hub management with intermittent wind power," in *Large Scale Renewable Power Generation*. Springer Singapore, 2014, pp. 413–438.

[28] T. Amraee, A. Soroudi, and A. Ranjbar, "Probabilistic determination of pilot points for zonal voltage control," *IET Generation, Transmission & Distribution*, vol. 6, no. 1, pp. 1–10, 2012.

[29] A. Conejo, F. Milano, and R. Garcia-Bertrand, "Congestion management ensuring voltage stability," *IEEE Transactions on Power Systems*, vol. 21, no. 1, pp. 357–364, 2006.

[30] K. Deb, *Multi-objective optimization using evolutionary algorithms*. Wiley, 2001, vol. 16.

[31] A. Soroudi, R. Caire, N. Hadjsaid, and M. Ehsan, "Probabilistic dynamic multi-objective model for renewable and non-renewable distributed generation planning," *IET Generation, Transmission & Distribution*, vol. 5, no. 11, pp. 1173–1182, 2011.

[32] A. Brook, D. Kendrick, and A. Meeraus, "Gams, a user's guide," *ACM SIGNUM Newsletter*, vol. 23, no. 3-4, pp. 10–11, 1988.

[33] P. E. Gill, W. Murray, and M. A. Saunders, "Snopt: An SQP algorithm for large-scale constrained optimization," *SIAM Review*, vol. 47, no. 1, pp. 99–131, 2005.

[34] A. J. 2010, "http://www.pserc.cornell.edu/matpower."

[35] M. Nick, G. Riahy, S. Hosseinian, and F. Fallahi, "Wind power optimal capacity allocation to remote areas taking into account transmission connection requirements," *Renewable Power Generation, IET*, vol. 5, no. 5, pp. 347–355, 2011.

[36] Y. E. S. El-Rayani, "Impact analysis models of renewable energy uncertainty on distribution networks," Ph.D. dissertation, University of Waterloo, 2012.

Abbas Rabiee received the B.Sc. degree in electrical engineering from Iran University of Science and Technology (IUST), Tehran, in 2006, and the M.Sc. and Ph.D. degrees in electrical power engineering from Sharif University of Technology (SUT), Tehran, Iran, in 2008 and 2013, respectively. Currently, he is with the Department of Electrical Engineering, Faculty of Engineering, University of Zanjan, Zanjan. Iran. His research interests include power system operation and security, and the application of optimization techniques in power system operation.

Alireza Soroudi (M14) Received the B.Sc. and M.Sc. degrees from Sharif University of Technology, Tehran, Iran, in 2002 and 2004, respectively, both in electrical engineering. and the joint Ph.D. degree from Sharif University of Technology and the Grenoble Institute of Technology (Grenoble-INP), Grenoble, France, in 2011. He is the winner of the ENRE Young Researcher Prize at the INFORMS 2013.

Behnam Mohammadi-Ivatloo (S09, M12) received the B.Sc. degree in electrical engineering from University of Tabriz, Tabriz, Iran, in 2006, the M.Sc. and PhD degree from the Sharif University of Technology, Tehran, Iran, in 2008, all with honors. He currently is an assistant professor with Faculty of Electrical and Computer Engineering, University of Tabriz, Tabriz, Iran. His main area of research is economics, operation and planning of intelligent energy systems in a competitive market environment.

Mostafa Parniani (Senior Member, IEEE) is an associate professor at Sharif University of Technology (SUT), Tehran, Iran. He received his B.Sc. degree from Amirkabir University of Technology, Iran, in 1987, and the M.Sc. degree from SUT in 1989, both in Electrical Power Engineering. He worked for Ghods-Niroo Consulting Engineers Co. and for Electric Power Research Center (EPRC) in Tehran during 1988-90. He obtained the Ph.D. degree in Electrical Engineering from the University of Toronto, Canada, in 1995. He was a visiting scholar at Rensselaer Polytechnic Institute, USA, during 2005-2006. His research interests include power system dynamics and control, applications of power electronics in power systems and renewable energies.